Adsorption of Hexavalent Chromium on Granular Activated Carbon fortified with a layered double hydroxide of Mg and Fe in aqueous solutions

Wang Xuejiang[1], Murigi Peter Njoroge[1]*, Li Yuan[1], Xia Siqing[1], Zhao Jianfu[1]

[1] State Key Laboratory of Pollution Control and Resource Reuse, School of Environmental Science and Engineering, Tongji University, Shanghai 200092, China

DOI: 10.29322/IJSRP.10.06.2020.p102125
http://dx.doi.org/10.29322/IJSRP.10.06.2020.p102125

Abstract- A novel Granular activated carbon and Manganese/Iron-layered double hydroxides (LDH) composite was synthesized by co-precipitation method. Layered double hydroxides (LDH) have remarkable adsorptive characteristics which includes ease of synthesis, porous structure, uniform dispersion of various metal cations in the brucite layer, surface hydroxyl clusters, adaptable tunability, intercalated anions with interlayer spaces, high chemical and thermal stability, capacity to intercalate different kinds of anions, conveyance of intercalated anions in a continued way and furthermore high biocompatibility.

The synthesized composite was subsequently used to adsorb Cr^{6+} from simulated wastewater diluted from potassium dichromate salt. Parameters such as initial pH, adsorbent dosage, reaction time and coexistence cations were investigated by batch experiments. Kinetics and isotherms studies showed that Cr^{6+} adsorption onto Mn/Fe-LDH-GAC followed Langmuir and pseudo second order models. The rate constant k_2 increased with solution pH. The highest adsorption value of Cr^{6+} on Mn/Fe-LDH-GAC was 17.001 mg/g while the value for non-modified GAC was 13.428mg/g. Compared to non-modified granular activated carbon, Mn/Fe-LDH-GAC exhibited a higher adsorption performance and potential applicability for removal of chromium from wastewater.

The results showed that layered double hydroxides of magnesium and iron to had a catalytic effect when fused with granular activated carbon, resulting in a composite adsorbent which showed improved performance. This novel adsorbent could therefore be scaled and applied for removal of the toxic hexavalent chromium ions from textile wastewater.

Index Terms- GAC, Mg/Fe-GAC-LDH, hexavalent chromium, adsorption, isotherms

I. Introduction

1.1 Significance of the research

Anthropogenic activities have increased in tandem with global population growth in the past few decades. Production of wastes has evolved along with the industrial growth. Most of these wastes are released in liquid form, otherwise referred to as wastewater which eventually finds its way into water bodies, exaggerating the already existing issue of freshwater shortage. There has thus existed a constant need to deal with wastewater as a big risk to ecosystems and human health and existence. The conventional methods to effectively remove contaminants from wastewater such as chemical-precipitation, membrane filtration such as reverse osmosis, ion-exchange, electrodialysis, and the adsorption methods have challenges ranging from low pollutant removal efficiency to high cost[1].

Therefore, the researcher proposes the synthesis of a composite adsorbent compound by calcining LDHs with GAC to combine the synergetic action of the two kinds of adsorbents to attain one that is has low cost, high adsorption capacity, and unique structure for removal of Chromium[2-4]. Different materials have been studied as suitable adsorbents to achieve removal of Chromium from aqueous solutions, including alumina and aluminum-based sorbents, calcium-based sorbents, carbon-based adsorbents. Notably, none of the previous researchers has conclusively focused on the possibility of attaining a more dynamic adsorbent by calcining LDHs with Activated Carbon, particularly the double hydroxide combination of magnesium and iron. This forms the basis of this research.

1.2 Application of Chromium in Textile Industry

Textile industry is a major producer of industrial wastewater globally. Treatment of wastewater deriving from textile districts is an issue of great environmental importance owing to the complexity of the removal of chemicals involved in this industrial process, and to their toxicity. Moreover, textile industry consumes a large quantity of water (about 10–50L) are required per kilogram of textile, depending on the type of processing), consequently producing large volumes of wastewater. Chromium complexed dyes are used as chromium salts in khaki dyeing[5-7]. Data from the textile industry indicates that chromium concentration increases 40 to 50 folds when a cloth is processed in this manner. Nonetheless, chromium concentration varies significantly from industry to industry depending on the extent and intensity of the dyeing process.

1.3 Effects of Chromium release to the environment

The contamination of environment by Chromium is a critical problem because of adverse effects on aquatic life and human health[3, 6, 8]. Cr^{3+} is a stable oxidation state and slowly reacts to form complexes. In view of its low motor vitality potential, Cr^{3+} is definitely not a solid oxidizer and apparently the

stomach's sharpness is sufficient to keep the Chromium in the Cr^{3+} state. Cr^{6+} isn't as steady as Cr^{3+} in light of the fact that it is a solid oxidizing operator, is quick responding, and likely structures edifices. Hexavalent chromium is all around considered to be a gathering "A" human cancer-causing agent in light of its mutagenic and cancer-causing properties. It is remembered for the need rundown of unsafe substances since it influences both; human and oceanic life. It has been likewise revealed that over the top admission of hexavalent chromium by plants seriously influences the mitotic procedure and decrease seed germination in widely developed pulse crops.

1.4 Factors influencing speciation of Chromium

Chromium speciation is controlled by two factors, namely pH and chromate concentration[9-11]. When the pH value is above 2, chromium ions exist in aqueous solution are as hexavalent chromate in the form of Cr_2O_7 pH 6.8, only CrO_4^{2-}, $HCrO^{4-}$, or/and CrO_4^{2-}. Above pH value of 2, $Cr^{6+}$is stable in solution, while the predominant species of Cr^{6+} in solution is $HCrO^{4-}$ as pH decreases into pH region 2∼6.8. Due to electrostatic repulsion, these Cr^{6+} oxyanions are by and large ineffectively adsorbed by contrarily charged soil particles; thus, they are exceedingly portable in oceanic environment. As a result, critical intrigued has been centered on inquire about into the expulsion of Cr^{6+} from waters. It's therefore of paramount importance to have a wastewater management system capable of ensuring water reuse for textile industrial districts more than for other kinds of industry. In order to achieve this goal, the quality level of the effluent must meet the stringent limits enforced by various authorities[12]

1.5 Granular Activated Carbon (GAC)

Granular enacted carbon (GAC) is broadly utilized as a compelling catalyst back due to its high porosity, expansive surface region, and tall catalytic action. Be that as it may, in arrange to improve its catalytic proficiency, the adjustment of GAC with dynamic chemicals has generally been explored, recommending that the new catalysts might evacuate heavy metals effectively. Moreover, GAC shows a few catalytic movements for evacuation of heavy metals due to its graphitic structure and the useful groups on their surface [13-15]. Whereas recent investigations have illustrated that both manganese oxide and GAC have high efficiencies and rates for the treatment of textile wastewater, studies on granular activated carbon coated with layered double hydroxides have not however been reported.

1.6 Layered Double Hydroxides

Layered double hydroxides (LDHs) are a kind of anionic clay with large anion sorption capacities. The general chemical composition of LDHs can be described as in the formula $[M^{2+}{}_{(1-\alpha)}N^{3+}(OH)_2]^{\alpha+}[A^{n-}]_{\alpha/n}\bullet mH_2O$, where M^{2+} is the divalent cation (Mg^{2+}, Zn^{2+}, Mn^{2+},Co^{2+}, Ni^{2+}, Cd^{2+}, etc.), N^{3+} is the trivalent cation (Al^{3+}, Fe^{3+}, Cr^{3+},Ga^{3+}, etc.), A^{n-} is the interlayer anion (CO_3^{2-}, SO_4^{2-}, NO^{3-}, Cl^-, OH^- ,etc.) and α is the $N^{3+}/(M^{2+}+N^{3+})$ ratio. LDHs are a host-guest material consisting of positively charged metal hydroxide sheets with intercalated anions and water molecules. In general, the value of x ranges between 0.17 and 0.33. Since of their positively charged brucite-like sheets and generally weak interlayer bonding,
LDH regularly show great affinity to different anions such as non-metal oxyanions, anionic metal complexes, natural anions and anionic polymers [11]. Layered double hydroxides (LDHs) have been broadly utilized within the adsorption process due to its special structure. The properties of the LDO such as high specific surface range, pore structure and recovery capacity make them more alluring in adsorption applications. One of the properties is "structure memory effect" by recreation of the LDO, where any accessible anion is absorbed into the interlayer spaces besides the anion that's within the unique LDH. Cr^{3+} acts as the counterbalancing anion for the LDO [11]. The capability of the LDO for the Cr^{6+} expulsion is influenced by numerous components such as fabric nature, specific surface area, pore structure and surface properties. Particularly, the LDH has high specific surface areas and is of great interest, having been found to improve the adsorption properties [12].

1.7 GAC impregnation with LDH

In this modification method, GAC is mixed with metal oxides or salts so that a physical or chemical attachment can be obtained with the metal ions remaining on the GAC. The impregnation can be in two different processes. The first is where soaking or suspending GAC in the metal oxides or salt solution is done, then followed by pyrolysis in temperature of between 300-900ºC. In the second case, pyrolysis comes first, then soaking, washing and drying.[13]. Several studies have proven that GAC containing several types of metallic oxides (CaO, MgO, Fe_2O_3, La_2O_3, and others) presents higher Chromium adsorption capacity than their original GAC[14]. Mg/Fe-GAC nanocomposites enhances removal of Chromium due to presence of MgO/Mg $(OH)_2$ nanosized particles within the matrix and surface charge alteration of GAC. GAC with impregnated nano-scale materials exhibits an improved removal of inorganic and organic contaminants by forming new sites like composites to increase yield and sorption sites for GAC. Nutrients contaminant removal by GAC is mainly through adsorption where the developed pore structure and large surface area provide sufficient space for adsorption which improves the process of mass transfer significantly. The use of modified GAC, both as a contaminant management and for treatment of textile wastewater [15], has gained considerable attention because it is abundantly available, economically and environmentally sustainable [16, 17].

II. METHODOLOGY

2.1 Chemicals and reagents

All the chemicals and reagents were purchased from reputable chemical companies in Shanghai and are of analytically pure grade as standardized by the required authorities.

2.2 Standard solutions

A stock solution of 100 mg/L chromium was prepared with the appropriately weighed amount of potassium dichromate.

Thereafter, standard solutions of the desired concentrations (5–30 mg/L) were obtained by appropriate dilutions of the stock solution. Double- distilled water was applied in the preparation all of the solutions and reagents. The initial pH was adjusted by adding 0.1 M HCl and 0.1 M NaOH. Adsorption experiments were performed at room temperature (25± 2 ºC). All the experiments were duplicated and the mean values recorded. Equation (1) is applied to prepare the stock solutions:

$$\frac{\text{Final conc(Mg/L)} \times \text{molecular weight of compound(gms)}}{\text{molecular weight of required molecule(gms)}} = \text{Weight of compound(gms)} \quad (\text{eq. 1})$$

2.3 Preparation of LDH-modified GAC

2.4g of Iron (III) chloride hexahydrate $FeCl_3$, 5.7g Magnesium chloride hexahydrate ($MgCl_2.6H_2O$) and 5g GAC were placed in a 250ml beaker. 200 ml deionized water was added and stirred for 1 hour with a magnetic stirrer. NaOH was used to adjust the solution pH to 13. The solution was stirred for 24 hours with a magnetic stirrer. Lastly, the sediments were washed, filtered and dried.

2.4 Characterization of samples

All synthesized materials were characterized by powder X-ray diffraction with the help of JCPDS sheets. X-ray diffractograms (XRD) was recorded by a diffractometer using Cu Ka radiation with a secondary graphite monochromator. The powder (1e50 mm) was used for determination. The diffraction intensity was observed between 5 and 70, with 2 steps. The hydrotalcite crystal size was calculated at diffraction line 23 and for calcined hydrotalcite at diffraction line 43 by utilizing the Scherrer equation D ¼ 0.9l/(bcosq); where D is the size of crystal (nm), 0.9 is the value of the utilized shape factor, I is the wavelength of the utilized Cu Ka radiation (0.154056 nm), b is the full width at half-maximum (FWHM) and q is the diffraction angle.

The chemical composition, i.e. the magnesium and iron con- tent in Mg-Fe calcined hydrotalcite, was determined using X-ray fluorescence - XRF (recorded with X-ray fluorescence spectrometer. The tablet for the measuring of XRF (voltage 50kV, current 20 mA) was prepared from 8g of cellulose and a 0.5g sample of mixed oxide, which was triturated. The basic fundamental parameters method without a calibration curve was used.

The surface area of samples was determined from the nitrogen adsorption-desorption isotherms at liquid nitrogen temperature (196^0C) and relative pressure (0.1, 0.15, 0.2,0.25 and 0.3) using XR equipment. The specific surface area (SBET) was determined by the fitting of the experimental data to the BET isotherm. The pore size distribution was estimated from adsorption branch of the finely measured isotherm using the original DFT method for slit shaped pores and N_2 adsorption at 196^0C.

Thermogravimetric analysis (TGA/MS) of dried HT catalysts
was gotten utilizing TA Instruments Discovery TGA working at a warming incline of 10^0Cmin-1 from room temperature to 900^0C with a steady flow of nitrogen (20 cm^3min^{-1}, Linde 3.0). Roughly 20 mg of the test was warmed in an open alumina ceramic cauldron (70 ml). Infrared spectra (32 scans; resolution of 1cm) was collected on a FTIR spectrometer equipped with an MCT/A detector. The samples were squeezed into self-supporting wafers with a thickness of approximately 10 mg/cm^2 and put into home-made IR cell designed for transmission estimation. The tests were outgassed in a dynamic vacuum at 450^0C up to residual pressure 104Pa. IR spectra of the CO_2 (purity 99.9993) surface complexes were collected at an equilibrium pressure of 100mbar at room temperature. Thereafter, the desorption at room temperature was performed in a dynamic vacuum at an elevated temperature of 100^0C. Desorption of CO_2 was realized to reveal the relative stability of the surface complexes. [18-23]
The metal ion content in solution were analyzed by inductively coupled plasma-optical emission spectrometry (ICP-OES, Agilent 720 ES)

2.5 Batch Adsorption Experiments

Batch series[1] experiments to remove Cr^{6+} through adsorption were performed in stoppered conical flasks of 250 mL capacity at room temperature. Determined amounts of adsorbents (0.4- 2.8 g) were added to the flasks containing 50 mL of chromium nitrate. The solutions were stirred in a mechanical shaker until equilibrium time is reached. Resultant solutions were sampled periodically, then filtered and the filtrate analyzed via atomic absorption spectrophotometry on the ICP machine. Effects of the initial pH, initial Cr^{6+} concentration, stirring time, and adsorbent dose on Cr^{6+} removal was evaluated. The design of the initial Cr^{6+} concentrations was in the 5-30 mg/L range. pH adjustment of the solution was achieved by adding drops of 0.1N sodium hydroxide or 0.1N hydrochloric acid solutions. Kinetic studies and adsorption isotherms were carried out with varying initial concentrations of the stock solutions in a standard adsorption as detailed in closely related previous studies

2.6 X- ray diffraction

(Figure 1 and 2) shows the crystal structure of the synthesized material Mg/Fe-LDH-GAC. The scanning angle (2θ) was between 10º and 90º. For GAC, the main diffraction peaks were found at scanning degree of 28º and 29º while those of Mg/Fe-LDH-GAC were 29.5,31,36,40,42.5,50,54.5,61,73 and 81º. The limited spectral bands in a GAC adsorbent in its natural state while has more spectral bands in the opened-up nanocrystals structure, opening up more adsorptive sites. This was in agreement with previous reports[24, 25]. Compared with that of GAC, the prepared Mg/Fe-LDH-GAC composite exhibited a typical hydrotalcite compound structure with the sharp reflection peaks.

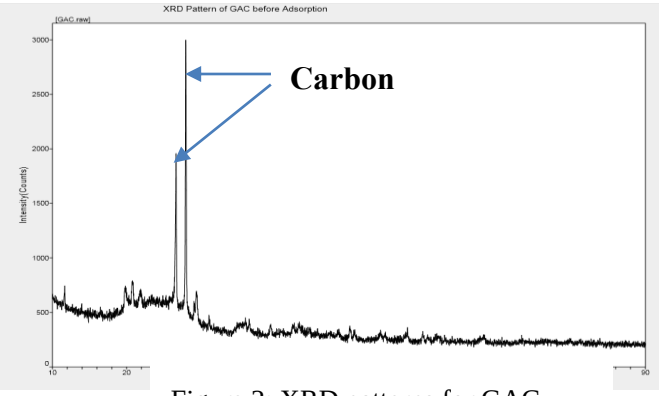

Figure 2: XRD patterns for GAC

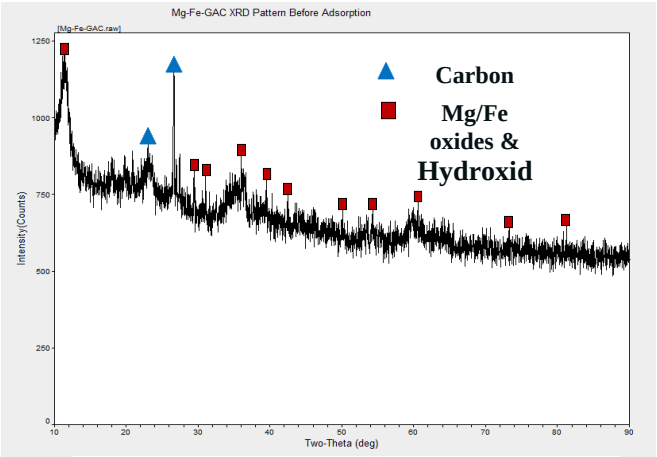

Figure 1: XRD patterns for Mg/Fe-GAC

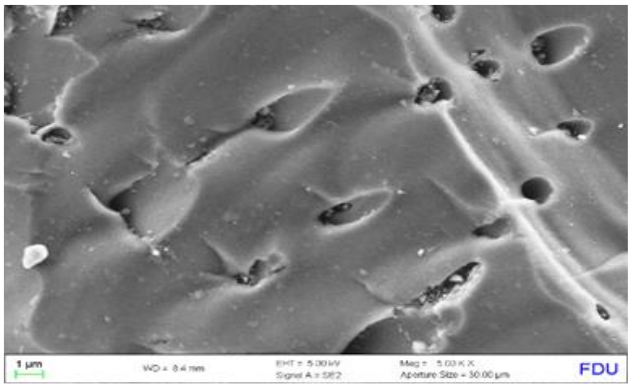

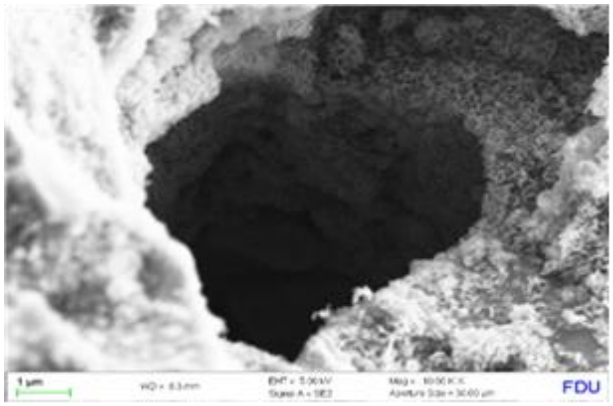

(b)

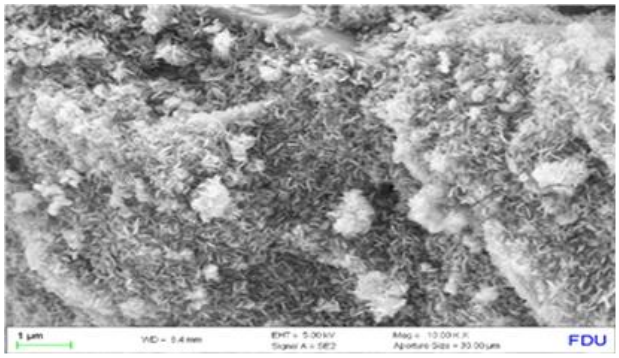

(c)

Fig 3**:** a) The surface morphology of GAC b) Mg/Fe-LDH-GAC respectively at 1µm c) Surface morphology of Mg/Fe-LDH-GAC at 200µm

2.7 Scanning Electron Micrograph

(Figure 3) details the SEM images of the synthesized adsorbents. The packed crystal formation with small pores gives GAC its adsorptive characteristics. The surface morphology of synthesized Mg/Fe-LDH-GAC composite exhibits a porous and nano-flakes surface are beneficial for the increase of GAC surface area and further improves adsorption; the size, amount, distribution and morphological structure of nano-particles is important in enhancing adsorption.

2.8 Fourier Transform infrared-radiation (FTIR)

The FTIR analysis was conducted on the Mg/Fe-LDH-GAC composite before and after hexavalent chromium adsorption (Figure 4). For the Mg/Fe-LDH-GAC composite sample before hexavalent chromium adsorption, the FTIR low frequency peaks centered at 1040cm^{-1} were assigned to the Fe–O or Mg-O band stretching vibrations, whereas the less intensive bands around 3650cm^{-1} peak was associated with stretching and bending modes of Fe-O. The peak at 1391 cm^{-1} was due to the translational mode of both Fe-OH and Mg-OH. The benzene ring C = C stretching peaks at 1459 and 1553 cm^{-1} indicated aromatization occurred during the biochar preparation. The broad bands located at 1631cm^{-1} and 3368 cm^{-1} were associated with the O−H stretching vibrations and H−O−H stretching and bending vibrations of the hydroxyl groups in the Mg/Fe-LDH-GAC composite or the adsorbed water molecules. After Mg/Fe-LDH-GAC composites were applied in adsorption of hexavalent chromium, the strength of Fe–O stretching vibration at 1040,1390 and 3450cm^{-1} reduced but could still be observed, confirming the involvement of Fe-O or Mg-O bonds in hexavalent chromium adsorption. The emergence of a strong asymmetry vibration peak at 1040cm^{-1} indicated that hexavalent chromium was strongly adsorbed by metal oxide surface (Mg–O and Fe-O) through the formation of potentially monodentate and bidentate inner-sphere surface complexes.

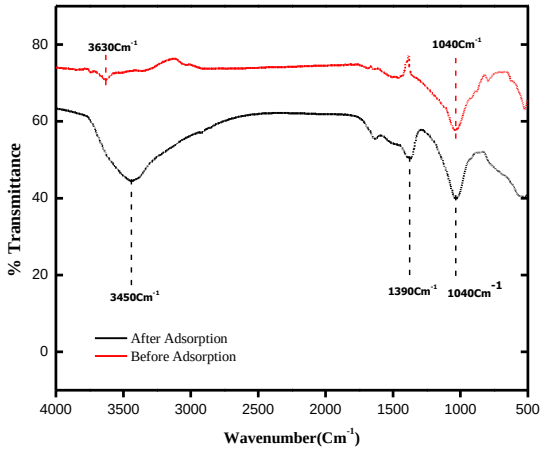

Figure 0: FT-IR spectra of Mg/Fe-LDH-GAC before and after adsorption

2.9 Adsorption performance

2.9.1 Effect of Contact time

To determine the equilibrium time of adsorption of hexavalent chromium ions onto GAC and Mg/Fe-LDH-GAC, 2g of each adsorbent were chosen to be used with 50 mg/L of simulated wastewater at room temperature 298K and pH 2. The contact time range was set from 5-120 minutes at initial intervals of 5min which was incrementally spaced to 30mins in the final interval.

It was found that the removal rate of Cr^{6+} continuously increases and then remained constant after 100 minutes. There was a dramatic increase of Cr^6 removal in the first 60 minutes for both adsorbents and slow till 120 minutes. This can be explained that there were numerous vacant surface sites for adsorption which seemed to be higher for Mg/Fe-LDH-GAC than GAC. As the time increased, the number of vacant sites available decreased and adsorption sites became saturated, leading to flattening of the curves after 60 and 70 mins respectively for GAC and Mg/Fe-LDH-GAC respectively as shown in (Figure 5).

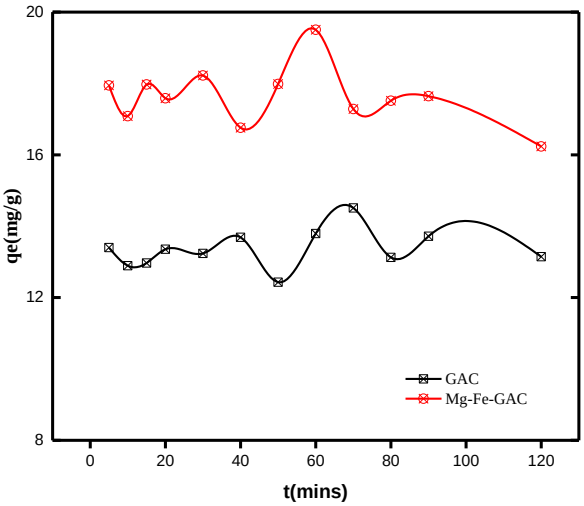

Figure 3: Effect of contact time on Cr^{6+} adsorption.

2.9.2 Effect of pH

The initial pH affects the charge distribution of the surface of the adsorbents as well as the dye molecules (adsorbate). To study the influence of pH on adsorption capacity of GAC and Mg/Fe-LDH-GAC, the experiments were performed in the pH range of 2-10 at 298K for 180 ppm with the pH of the aqueous solutions adjusted using 0.1M HCl and 0.1 M NaOH solutions. As shown in (Figure 6), starting from pH of 2, the adsorption capacity for and attains the maximum at pH 2 and pH 5 for GAC and Mg/Fe-LDH-GAC respectively. This was due to the electrostatic interaction between positively charged surface of the adsorbent and anionic dichromate ions in the simulated textile wastewater. Lower adsorption values for both adsorbents at higher pH may be described by the competition for active sites by increasing OH^- ions with Cr^{6+} anions for the adsorption sites. This situation was evident at pH range 6-10. Diminished rate of removal of Cr^{6+} continues in the pH range 6-10 which could be due to the formation of aqua cationic species from Cr^{6+} in solution due to its hydrolysis and the removal may not be due to adsorption. There, GAC depicted optimum performance removal at pH value of 5 while Mg/Fe-LDH-GAC performed best at low pH of 2 in an acidic environment, where the metallic cations of Mg^{2+} and Fe^{3+} contributed in increasing acidity in the aqueous environment (Table 1)

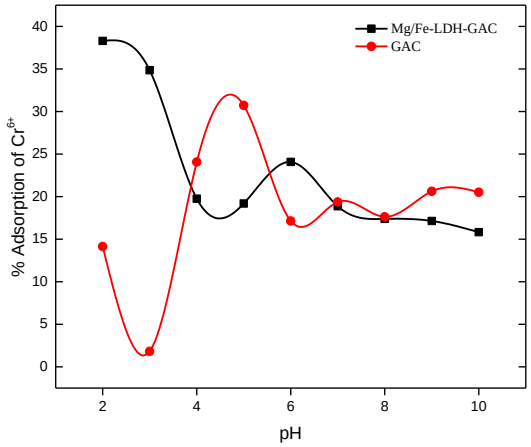

Figure 4: Effect of pH on Cr^{6+} adsorption by GAC and Mg/Fe-LDH-GAC, 60 min, 180 rpm at 298 K.

Table 1: Cr^{6+} pH optimization for different adsorbents

Types of adsorbent	Optimized pH	References
MgO nanostructure	2	[26]
Hematite	3	[27]
Dried powdered biomass (Chlorella Vulgaris Beijerinck)	5	[28]
MgO nanoparticle	3	[29]
Modified chitosan beads	3	[30]
GAC	5	This study
Mg/Fe-LDH-GAC	2	This study

2.9.3 Effect of adsorbent dose

Adsorbent dosage is another important factor affecting the adsorption process through determining the amount of adsorbate removed. In this study, the effect of adsorbent on removal of Cr^{6+} ions from aqueous solution was determined by changing the doses of GAC and Mg/Fe-LDH-GAC adsorbents from 0.4 to 2.8 g at 298K, mixed at 180 rpm on the electromagnetic stirrer for a contact time of min and at varying Cr^{6+} ions concentration of 5 to 30 mg/L. The optimum adsorbent concentration was determined to be 2 mg/L. Moreover, (figure 8) indicates that the removal efficiency of Cr^{6+} ions increased at an average value of 46.47% when Mg/Fe-LDH-GAC was used in place of GAC with a noted increase in performance ratio with increasing initial concentration of the Cr^{6+} ions in the aqueous solution as shown in (Figure 7). There is a notable discrepancy between the binding sites and holding capacity of the adsorbents makes them less efficient towards removal Cr^{6+} ions at low adsorbent dosage. However, when the adsorbent dosage is increased, more surface area will be available hence due to the increased active sites since more Cr^{6+} ions are retained by the excess surface centers. Therefore, adsorbent dosage of 2.0 g was chosen for the subsequent studies.

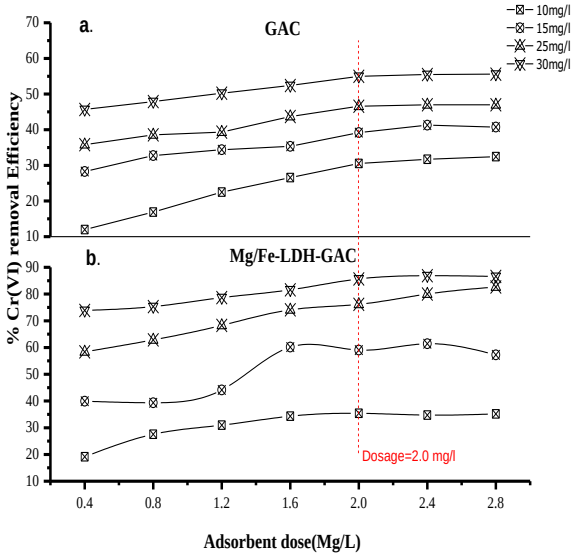

Figure 5: Effect of adsorbents dosage on Cr^{6+} removal.

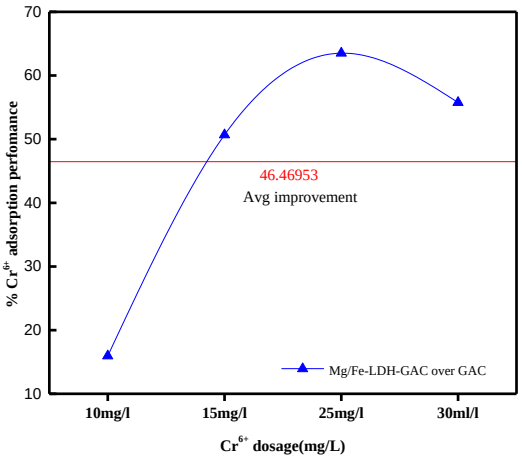

Figure 6: Performance of Mg/Fe-LDH-GAC over GAC.

2.9.4 Effect of initial Cr^{6+} concentration

The effect of initial hexavalent chromium concentration on adsorption capacity of GAC and Mg/Fe-LDH-GAC adsorbents was investigated at a concentrations 50 mg/L by keeping other parameter constant (adsorbent dose of 2 g, pH=2 for Mg/Fe-LDH-GAC and pH=5 for GAC,2h min, 180 rpm with at 298 K). It was found that the adsorption capacity was increasing with commensurate increasing initial concentrations. This can be explained that there were sufficient binding sites available for Cr^{6+} adsorption, which resulted to a maximum interaction between Cr^{6+} and the adsorbent.

2.9.5 Adsorption isotherms

Isotherm studies offer significant insights by clarifying the adsorbate distribution between solid and liquid phases in the process of adsorption equilibrium. This helps to reveal the actual adsorbate behavior in presence of novel adsorbent such as the one applied in this study (Mg/Fe-LDH-GAC). To achieve a more detailed study of the adsorption mechanism for GAC and Mg/Fe-

LDH-GAC, adsorption data for Cr^{6+} ions was fitted by the Langmuir and Freundlich isotherm models as described in the sections below and presented in (Figure 9 and 10) respectively. The high correlation coefficient (R^2) values of the adsorbent applied indicated that the experimental data of both GAC and Mg/Fe-LDH-GAC fitted well to the Langmuir model with Mg/Fe-LDH-GAC giving a more favorable adsorption performance with R^2 value of 0.9953 compared with 0.9902 for GAC. Based on the hypothesis condition of Langmuir model, it was inferred that the adsorbate (Cr^{6+} ions) underwent monolayer chemisorption on the active sites on the surfaces of the adsorbents under comparative review (GAC and Mg/Fe-LDH-GAC). It is more appropriate to interpret that monolayer and multilayer adsorption processes both occur on the heterogeneous Mg/Fe-LDH-GAC but the monolayer chemisorption was most prevalent. (Table 4.3) shows that the theoretical maximum adsorption capacity (q_{max}) obtained from Langmuir model was 29.8507 mg/g, which was higher than that of GAC at 20.9293 mg/g.

a) **The Langmuir isotherm model,** which is derived on the assumption of monolayer adsorption on a homogeneous surface without any interaction between adsorbed molecules. It is represented in the equation (2).

$$\frac{C_e}{q_e} = \frac{C_e}{q_{max}} + \frac{1}{K_L\ q_{max}} \quad (eq.\ 2)$$

Where q_e, is the monolayer adsorption capacity(mg/g), Ce is the equilibrium concentration (mg/L), q_m is the maximum adsorption capacity that can be taken up per mass of adsorbent(mg/g) and K_L is the Langmuir equilibrium constant($L.mg^{-1}$). The maximum adsorption capacity(q_m) and K_L were determined from the slope and intercept of a plot of c_e/q_e against C_e, respectively in (Figure 4.9). The dimensionless separation factor R_L indicates the nature of adsorption (Whether the adsorption process is favorable or unfavorable) When the value of $R_L > 1$, the adsorption process is unfavorable; linear, when $R_L = 1$; favorable when $0 < R_L < 1$; and irreversible when $R_L = 0$.

The Langmuir model makes a presumption of monolayer adsorption onto the adsorbent dosage that is homogeneous in an adsorption process. It's also worth noting that a free energy change for all adsorption sites is uniform. Consequently, adsorption happens when the surface of the adsorbent applied is covered by a monolayer of adsorbate.

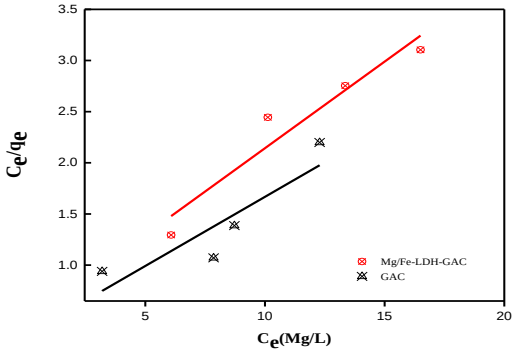

Figure 7: Langmuir isotherm for adsorption of Cr^{6+} onto GAC and Mg/Fe-LDH-GAC for 2h at 298 K.

b) **Freundlich isotherm** model assumes that the adsorption process occurs in a multiplayer manner over a heterogeneous surface with sites of diverse affinities. The well-known linear form of Freundlich isotherm is in the form:

$$\ln q_e = \ln K_f + \frac{1}{n}\ln C_e \quad (eq.\ 3)$$

Where, q_e, is the amount of either amount OG adsorbed at equilibrium(mg/g) and C_e is the equilibrium concentration of Cr^{6+} (mg/L). K_F [$(mg\cdot g^{-1})$ $(L\cdot mg^{-1})1/n$] is a rough indicator of the adsorption capacity as well as strength of adsorptive bond and n is Freundlich constant which represent the adsorption intensity (heterogeneity factor that represents the bond distribution. The values of K_F and n were calculated from the intercept and slope of the plot of ln q_e versus ln C_e respectively. The values of K_F and n as well as correlation R^2 are presented in (table 2).

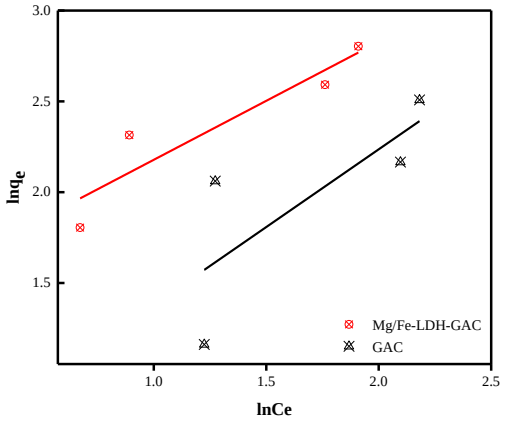

Figure 8: Freundlich isotherm for adsorption of Cr^{6+} onto GAC and Mg/Fe-LDH-GAC with 5-30 mg/L Cr^{6+} for 2h at 298 K

Table 2: Isotherm parameters for adsorption of Cr^{6+} onto GAC and Mg/Fe-LDH-GAC at 298 K for 5 h

Adsorption Isotherm	Parameter	Sample	
		GAC	Mg/Fe-LDH-GAC
Langmuir	K_L (L mg^{-1})	0.1157	0.0822
	q_{max} (mg-sg^{-1})	20.9293	29.8507
	R^2	0.7002	0.8910
Freundlich	K_F	3.3438	33.8314
	n	1.9824	5.4804
	R^2	0.9902	0.9953

2.9.6 Adsorption Kinetics

In order to understand and provide important information about the adsorption mechanism and dynamics, the two well-known kinetic models pseudo-first and pseudo-second order equations have been used to evaluate the adsorption mechanism of GAC and LDH-GAC composite on simulated wastewater containing Cr^{6+} ions. The pseudo-first order equation assumes adsorption of one adsorbate molecule onto one active site while

the pseudo-second-order equation assumes that one adsorbate molecule is adsorbate onto two active sites on the adsorbent surface. The equation (3) and (4) are the linear forms of pseudo-first and pseudo-second order equations, respectively.

$$ln(q_e - q_t) = lnq_e - k_1 t (eq.3) \text{ and}$$
$$\frac{t}{q_t} = \frac{1}{k_2 q_e^2} + \frac{t}{q_e} \ (eq.4)$$

Where qe is the amount adsorbed at equilibrium (mg/g), qt is the amount adsorbed at time t(mg/g), t is adsorption time(min), k_1 is the rate constant of pseudo-first order kinetic (g/mg/min), and k_2 is the rate constant of the pseudo-second-order kinetic (g/mg min).

a) Pseudo first order kinetics

The rate constant of pseudo-first order was determined from the pseudo-first linear equation $\ln(q_e-q_t) = \ln q_e - k_1 t$. The values of $k_1$and q_e are determined from the slope and intercept of the plot of $\ln(q_e-q_t)$ versus t, respectively. Their values as well as the linear regression (R^2) are shown in (Table 8). It was found that the linear regression coefficient (R^2) values obtained with this model are small and the values of calculated q_e are quietly differ from the experimental values. Therefore, the pseudo-first order didn't fit the experimental data (figure 11).

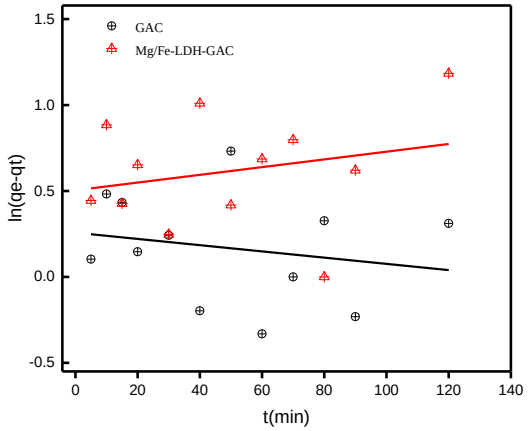

Figure 9: Pseudo first order kinetic adsorption of GAC and Mg/Fe-LDH-GAC for 50 mg/L Cr^{6+}, 2 g of adsorbent,

Adsorption Kinetic	Parameter	Sample	
		GAC	Mg/Fe-LDH-GAC
Pseudo-first order	k_1 (mg min g−1)	1.9349	1.5565
	q_e (mg g−1)	11.8085	33.1919
Pseudo-second order	k_2 (mg min g−1)	0.0409	0.0323
	q_e (mg g−1)	43.4282	77.0010
	R^2	0.98904	0.99529

pH=2(Mg/Fe-LDH-GAC) and pH=5(GAC), 60 min ,180 rpm at 298 K.

b) Pseudo-second-order

Adsorption kinetics is one of the most important factors in evaluating the efficiency of an adsorbent. The Chromium (VI) adsorption by the Mg/Fe-LDH-GAC composite as a function of time is presented in (figure 12). It is clear that initially hexavalent chromium adsorption was fast followed by a relatively slow adsorption, which is similar to other studies. The Cr^{6+} ions adsorption increased with extended contact time, was removed within 60 min. It was found that the correlation coefficients of the pseudo-second-order rate model for the linear relation of t versus t/qt was very close to 1 at R^2=0.9953 for the novel composite (Mg/Fe-LDH-GAC). This confirmed that Cr^{6+} had been adsorbed via chemical reactions. And also, the relevant parameters and normalized standards shown in (Table 3) concluded in favor of pseudo-second-order model which, without doubt, fitted the experimental data for the adsorption of Cr^{6+} onto GAC and Mg/Fe-LDH-GAC. In addition, q_e values obtained from the experiment (q_{exp}) were very closed to the calculated q_e values from this model. had been adsorbed via chemical reactions(chemisorption). And also, the relevant parameters and normalized standards shown in (Table 3). It can be concluded that the pseudo-second-order model undoubtedly fitted the experimental data for the adsorption of Cr^{6+} onto GAC the Mg/Fe-LDH-GAC. Furthermore, qe values obtained from the experiment (q_{exp}) were very closed to the calculated q_e values from this model. The initial rapid adsorption might be due to the electrostatic attraction between the positive charged metal oxide surfaces and the positively charged Cr^{6+} ions. The later slow adsorption indicated that intraparticle diffusion may be involved. The kinetic data of Cr^{6+} ions adsorption was also fitted with pseudo-first-order and pseudo-second-order kinetic model. The obtained kinetic models' parameters are listed in (Table 4.3). It was found that the Cr^{6+} ions adsorption could be better described by the pseudo-second-order kinetic model since the correlation coefficient (R^2) was higher than that of pseudo first-order kinetic model. These results were consistent with chemical behaviors of Cr^{6+} ions adsorption exhibited by other metal oxides and LDHs-based as listed in (Table 3)

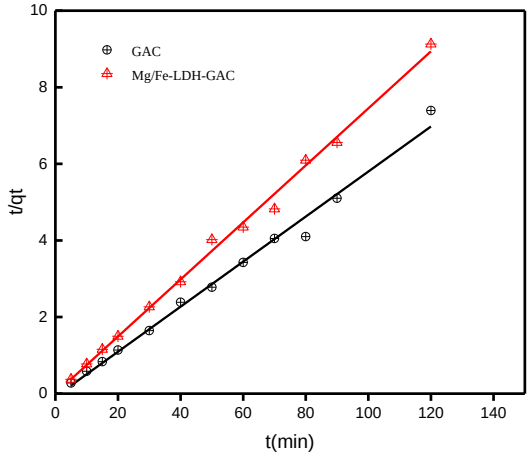

Figure 10: Pseudo second order kinetic adsorption of GAC and Mg/Fe-LDH-GAC Cr^{6+}, 2 g of adsorbent, pH=5 and pH=2 respectively, 60 min ,1800 rpm at 298 K.

Table 3: Kinetic parameters

.

III. Conclusion

This study concluded that LDH/GAC composites, which can be synthesized through liquid phase co-precipitation of LDH on GAC matrix, may provide a novel absorbent for treatment of Chromium-laden waters. The Mg/Fe-LDH-GAC composites had higher Hexavalent Chromium adsorption with adsorption enhancement of adsorption by more than 40%. The SEM images revealed that GAC served as an effective matrix for LDH to deposit on, thereby creating a synergistic effect between LDH and GAC in enhancing adsorption of Cr^{6+}. Experiments on batch adsorption indicated that the 40% Mg/Fe-LDH-GAC composite exhibited excellent Cr^{6+} adsorption capacity with a commendable adsorption time of less than an hour when applied at typical concentrations found in textile wastewater. The XRD and XPS spectra singled out surface adsorption and interlayer anion exchange to be the main Cr^{6+} removal processes. The adsorption isotherm suggested precipitation mechanism as another possible adsorption mechanism at higher hexavalent chromium concentration which agrees with previous studies. Results from this study can be applied in the development of a cheaper and sustainable way to develop and apply the LDH-modified GAC to reclaim Cr^{6+} in both potable water and wastewaters streams as well as a way to recycle it back to soils to improve food production and fix carbon. Future research can be conducted with column adsorption experiments to test the efficiency of the material in a filtration bed setting.

References

[1] [1] B. D. G. M. A. Mary Lissy P N, "Removal of Heavy Metals from Waste Water Using Water Hyacinth," ACEEE International Journal on Transportation and Urban Development, vol. 1, no. 1,April 2011, 2011.

[2] [2] H. O. Y. Terashima, M. Sekine, "Removal Of Dissolved Heavy Metals By Chemical Coagulation, Magnetic Seeding And High Gradient Magnetic Filtration," Water Resources, vol. 20, no. 5, pp. 537-54, 1986.

[3] [3] A. B. S. Mustafiz, M. R. ISLAM, "A Novel Method for Heavy Metal Removal," Energy Sources, vol. 24, pp. 1043–1051, 2002.

[4] [4] M.-K. S. Chang-Gu Lee, Jae-Chun Ryu, Chanhyuk Park, Jae-Woo Choi, and S.-H. Lee, "Application of carbon foam for heavy metal removal from industrial plating wastewater and toxicity evaluation of the adsorbent," Chemosphere, vol. 153, pp. 1-9, 2016.

[5] [5] G. M. Walker and L. R. Weatherley, "Textile Wastewater Treatment Using Granular Activated Carbon Adsorption in Fixed Beds," Separation Science and Technology, vol. 35, no. 9, pp. 1329-1341, 2000.

[6] [6] S. Y. R. Fahmida Parvin, Shafi M. Tareq, "Application of Nanomaterials for the Removal of Heavy Metal From Wastewater," Nanotechnology In Water And Wastewater Treatment, 2018.

[7] [7] B. Ranjan, S. Pillai, K. Permaul, and S. Singh, "Simultaneous removal of heavy metals and cyanate in a wastewater sample using immobilized cyanate hydratase on magnetic-multiwall carbon nanotubes," J Hazard Mater, vol. 363, pp. 73-80, Feb 5 2019.

[8] [8] D. Cetin, S. Donmez, and G. Donmez, "The treatment of textile wastewater including chromium(VI) and reactive dye by sulfate-reducing bacterial enrichment," J Environ Manage, vol. 88, no. 1, pp. 76-82, Jul 2008.

[9] [9] G. S. J. Aravind, P. Kanmani,A.J. Devisri, S. Dhivyalakshmi, M. Raghavprasad, "Equilibrium and kinetic study on chromium (VI) removal from simulated waste water using gooseberry seeds as a novel biosorbent," Global J. Environ. Sci. Manage, vol. 1, no. 3, pp. 233-244, 2015.

[10] [10] J. Huang et al., "Influence of pH on heavy metal speciation and removal from wastewater using micellar-enhanced ultrafiltration," Chemosphere, vol. 173, pp. 199-206, Apr 2017.

[11] [11] F. Y. Jinhui Huang, Guangming Zeng, Xue Li, Yanling Gu, and W. L. Lixiu Shi, Yahui Shi, "Influence of pH on heavy metal speciation and removal from wastewater using micellar-enhanced ultrafiltration," Chemosphere, vol. 173, pp. 199-206, 2017.

[12] [12] Standard Methods for the examination of Water and Wastewater, 1985.

[13] [13] M. Ahmad et al., "Speciation and phytoavailability of lead and antimony in a small arms range soil amended with mussel shell, cow bone and biochar: EXAFS spectroscopy and chemical extractions," Chemosphere, vol. 95, pp. 433-41, Jan 2014.

[14] [14] Q. Yin, B. Zhang, R. Wang, and Z. Zhao, "Biochar as an adsorbent for inorganic nitrogen and phosphorus removal from water: a review," Environ Sci Pollut Res Int, vol. 24, no. 34, pp. 26297-26309, Dec 2017.

[15] [15] K. Y. Chan, L. Van Zwieten, I. Meszaros, A. Downie, and S. Joseph, "Agronomic values of greenwaste biochar as a soil amendment," Soil Research, vol. 45, no. 8, pp. 629-634, 2007.

[16] [16] P. A. W. Mahardika Prasetya Aji, Jotti Karunawan, Annisa Lidia Wati,and Sulhadi, "Removal of Heavy Metal Nickel-Ions from Wastewaters Using Carbon Nanodots from Frying Oil," Engineering Physics International Conference, EPIC 2016, vol. 170, pp. 36 – 40, 2017.

[17] [17] W.-J. Liu, H. Jiang, and H.-Q. Yu, "Development of Biochar-Based Functional Materials: Toward a Sustainable Platform Carbon Material," Chemical Reviews, vol. 115, no. 22, pp. 12251-12285, 2015.

[18] [18] C.-R. Chen, H.-Y. Zeng, S. Xu, X.-J. Liu, H.-Z. Duan, and J. Han, "Preparation of mesoporous material from hydrotalcite/carbon composite precursor for chromium(VI) removal," Journal of the Taiwan Institute of Chemical Engineers, vol. 70, pp. 302-310, 2017.

[19] [19] R. Elmoubarki et al., "Ni/Fe and Mg/Fe layered double hydroxides and their calcined derivatives: preparation, characterization and application on textile dyes removal," Journal of Materials Research and Technology, vol. 6, no. 3, pp. 271-283, 2017.

[20] [20] G. Lee, J. Y. Kang, N. Yan, Y.-W. Suh, and J. C. Jung, "Simple preparation method for Mg–Al hydrotalcites as base catalysts," Journal of Molecular Catalysis A: Chemical, vol. 423, pp. 347-355, 2016.

[21] [21] S. Wan, S. Wang, Y. Li, and B. Gao, "Functionalizing biochar with Mg–Al and Mg–Fe layered double hydroxides for removal of phosphate from aqueous solutions," Journal of Industrial and Engineering Chemistry, vol. 47, pp. 246-253, 2017.

[22] [22] T. Wang, C. Li, C. Wang, and H. Wang, "Biochar/MnAl-LDH composites for Cu (II) removal from aqueous solution," Colloids and Surfaces A: Physicochemical and Engineering Aspects, vol. 538, pp. 443-450, 2018.

[23] [23] H.-Y. Zeng, X. Deng, Y.-J. Wang, and K.-B. Liao, "Preparation of Mg-Al hydrotalcite by urea method and its catalytic activity for transesterification," AIChE Journal, vol. 55, no. 5, pp. 1229-1235, 2009.

[24] [24] M. Laipan et al., "From spent Mg/Al layered double hydroxide to porous carbon materials," J Hazard Mater, vol. 300, pp. 572-580, Dec 30 2015.

[25] [25] Y. Wang, D. Zhang, and Z. Lu, "Hydrophobic Mg–Al layered double hydroxide film on aluminum: Fabrication and microbiologically influenced corrosion resistance properties," Colloids and Surfaces A: Physicochemical and Engineering Aspects, vol. 474, pp. 44-51, 2015.

[26] [26] L. L. M. F. Raquel P. D. Victor, Antônio A. Neves, Maria E. L. R. de Queiroz, André F. de Oliveira and Liany D. L. Miranda, , "Removal of Orange G Dye by Manganese Oxide Nanostructures, J. Braz. Chem. Soc., Vol. 30, No. 8, 1769-1778, 2019.."

[27] [27] S. S. Monoj Kumar Mondal, Meka Umareddy, Betty Dasgupta. , "Removal of Orange G from aqueous solution by hematite: Isotherm and mass transfer studies. Korean J. Chem. Eng., 27(6), 1811-1815 (2010).".

[28] [28] A. S. A. a. M. U. C. Sunil Kumar1, "Adsorption of Orange-G dye by the dried powdered biomass of Chlorella vulgaris Beijerinck, Current Science, Vol. 116, No. 4, 25 February 2019.."

[29] [29] F. Amir, Dawood, Abd, A., Khudheir, A, and Marwa, I., Mubarak, (2017). , "Study Eosin Dye Adsorption on the Surface Waste of Molasses Dates Production. Diyala Journal for pure sciences, 13(1), 22-41. ."

[30] [30] M. S. Zetty Azalea Sutirman, Khairil Juhanni Abd Karim, Ahmedy Abu Naim, Wan Aini Wan Ibrahim, , "Enhanced removal of Orange G from aqueous solutions by modified chitosan beads: Performance and mechanism. International Journal of Biological Macromolecules 133 (2019) 1260–1267.."

AUTHORS

First Author – Wang Xuejiang, State Key Laboratory of Pollution Control and Resource Reuse, School of Environmental Science and Engineering, Tongji University, Shanghai 200092, China
Second Author – Murigi Peter Njoroge, State Key Laboratory of Pollution Control and Resource Reuse, School of Environmental Science and Engineering, Tongji University, Shanghai 200092, China
Third Author – Li Yuan, State Key Laboratory of Pollution Control and Resource Reuse, School of Environmental Science and Engineering, Tongji University, Shanghai 200092, China
Fourth Author – Xia Siqing, State Key Laboratory of Pollution Control and Resource Reuse, School of Environmental Science and Engineering, Tongji University, Shanghai 200092, China
Fifth Author – Zhao Jianfu, State Key Laboratory of Pollution Control and Resource Reuse, School of Environmental Science and Engineering, Tongji University, Shanghai 200092, China

Corresponding Author: Murigi Peter Njoroge.
Address: UNEP- Tongji Institute of Environment for Sustainable Development, Department of Environmental Science, College of Environmental Science and Engineering, Tongji University Shanghai. 20092, China. Email: pnmurigi@gmail.com